Identification and characterization of photomedins: novel olfactomedin-domain-containing proteins with chondroitin sulphate-E-binding activity

Yutaka FURUTANI*, Ri-ichiroh MANABE*, Ko TSUTSUI*, Tomiko YAMADA*, Nagisa SUGIMOTO*, Shiro FUKUDA†, Jun KAWAI†, Nobuo SUGIURA‡||, Koji KIMATA‡, Yoshihide HAYASHIZAKI† and Kiyotoshi SEKIGUCHI*¶[1]

*Sekiguchi Biomatrix Signaling Project, Exploratory Research for Advanced Technology (ERATO), Japan Science and Technology Agency, Aichi Medical University, Nagakute, Aichi, 480-1195, Japan, †Genome Exploration Research Group, RIKEN Genomic Sciences Center, RIKEN Yokohama Institute, Yokohama 230-0045, Japan, ‡Institute for Molecular Science of Medicine, Aichi Medical University, Nagakute, Aichi 480-1195, Japan, ||Central Research Laboratories, Seikagaku Corporation, Higashiyamato, Tokyo 207-0021, Japan, and ¶Institute for Protein Research, Osaka University, Suita, Osaka 565-0871, Japan

We screened more than 60 000 RIKEN mouse cDNAs for novel ECM (extracellular matrix) proteins by extensive computational screening followed by recombinant expression and immunohisto-chemical characterization. We identified two novel olfactomedin-family proteins characterized by the presence of tandem CXCX-CX$_9$C motifs in the N-terminal region, a coiled-coil domain and an olfactomedin domain in the C-terminal region. These proteins, named photomedin-1 and photomedin-2, were secreted as di-sulphide-bonded dimers (photomedin-1) or oligomers/multimers (photomedin-2) with O-linked carbohydrate chains, although photomedin-1 was proteolytically processed in the middle of the molecule after secretion. In the retina, photomedin-1 was selectively expressed in the outer segment of photoreceptor cells and photomedin-2 was expressed in all retinal neurons. Among a panel of ECM components, including glycosaminoglycans, photomedins preferentially bound to chondroitin sulphate-E and heparin. These results, together, indicate that photomedins are novel olfactomedin-domain-containing extracellular proteins capable of binding to proteoglycans containing these glycosamino-glycan chains.

Key words: chondroitin sulphate-E, heparin, myocilin, olfacto-medin, retina.

INTRODUCTION

OLF (olfactomedin)-family proteins are an emerging group of extracellular glycoproteins characterized by the presence of an OLF domain in their C-terminal regions. The OLF domain is defined as an approx.-260-amino-acid sequence sharing homo-logy with the C-terminal region of OLF, a major component of the extracellular mucus matrix of olfactory neuroepithelium [1]. OLF-family proteins include noelins [2,3], tiarin [4], amassin [5], myocilin [6,7], optimedin/noelin-3 [8] and CIRL (calcium-inde-pendent receptor for α-latrotoxin)/latrophilin [9]. All except amassin are expressed in neural tissues and are implicated in the growth and differentiation of chemosensory cilia [1], early neuro-genesis [2,3], dorsalization of neural tubes [4], neuromuscular signalling [10], exocytosis of synaptic vesicles [11] and the patho-genesis of glaucoma [12–14]. However, the molecular mechan-isms by which OLF-family proteins exert their functions remain largely unknown.

The N-terminal region of OLF-family proteins is typically characterized by the presence of the leader sequence for protein secretion, followed by the CXC motif which is involved in disul-phide-bonded homodimerization/oligomerization [1]. The C-ter-minal OLF domain has also been implicated in dimerization/oligomerization [15]. Disulphide-bonded aggregate formation is critical for the activity of amassin, a coelomic plasma protein of the purple sea urchin (*Strongylocentrotus purpuratus*), to induce a massive intercellular adhesion of coelomocytes [5,16,17].

Recent progress in genome and transcriptome research makes it possible to screen for novel proteins having homology with known proteins through computational homology searches. Kulkarni et al. [18] identified five human OLF-family proteins through a homology search of the GenBank™ database. In an attempt to comprehensively identify novel ECM (extracellular matrix) proteins, we computationally screened RIKEN (Rikagaku Kenkyusho, The Institute of Physical and Chemical Research) full-length mouse cDNA collections (http://fantom2.gsc.riken.jp) for novel secreted proteins, followed by the expression of selected cDNAs as GFP (green fluorescent protein) fusions in a panel of cultured mammalian cells to examine their secretion and deposition into the ECM. Among the novel ECM proteins thus identified are two closely related OLF-domain-containing proteins that we have named photomedin-1 and photomedin-2.

Here we report the structure of these photomedins, their post-translational modification, including O-glycosylation and proteo-lytic processing, and their tissue localization in the retina. Although the functions of photomedins remain to be defined, both proteins are capable of binding to CS-E (chondroitin sulphate-E) and heparin and are strongly expressed in the retina in mutually exclusive patterns.

EXPERIMENTAL

Computational screening of novel ECM proteins

The RIKEN full-length cDNA collections were used as the source for sequence analysis. Putative secreted proteins were selected by PSORT II [19] (http://psort.nibb.ac.jp/). The presence of transmembrane domain(s) was predicted by SOSUI [20]. A homology search using FASTY [21] was used to eliminate any known proteins.

Cell culture

HEK-293T cells were maintained in Dulbecco's modified Eagle's medium supplemented with 10 % (v/v) FBS (fetal-bovine serum) at 37 °C in a humidified atmosphere containing 5 % CO_2. Freestyle™ 293F cells (Invitrogen, Carlsbad, CA, U.S.A.) were maintained in FreeStyle™ 293 Expression Medium (Invitrogen) according to the manufacturer's instruction.

Antibodies and fluorescent probes

Antibodies and fluorescent probes used were anti-(GFP B2) from Santa Cruz Biotechnology (Temecula, CA, U.S.A.), Alexa Fluor 488-conjugated goat polyclonal anti-rabbit IgG, Alexa Fluor 546-conjugated goat polyclonal anti-mouse IgG and propidium iodide from Molecular Probes (Eugene, OR, U.S.A.), anti-(FLAG M2) antibody from Sigma (St. Louis, MO, U.S.A.) and anti-rabbit IgG horseradish-peroxidase-conjugated F(ab')$_2$ fragment from Amersham Biosciences (Piscataway, NJ, U.S.A.).

Northern Blotting

Mouse multiple tissue blots were purchased from Seegene (Seoul, Korea), each lane containing 20 μg of total RNA. cDNA fragments derived from 3'-non-coding regions of photomedins were used as probes. Mouse GAPDH (glyceraldehyde-3-phosphate dehydrogenase) cDNA (554 bp) was also used as a control probe. Hybridization was performed by following a standard protocol [22].

Expression of GFP fusion proteins and FLAG-tagged proteins

For expression of GFP fusion proteins and FLAG-tagged proteins of photomedin-1 and -2, and FLAG-tagged albumin (designated PM1–GFP, PM2–GFP, PM1–FLAG, PM2–FLAG and albumin–FLAG respectively, where PM is photomedin), the coding regions, including their Kozak sequences, were amplified by PCR and subcloned into eukaryotic expression vectors, pCIkana-EGFP-3×myc and pFLAG-CMV5 (Sigma). The primers used were 5'-CCGGAATTCGCAGCCATGGAAGCGGC-AGCTG-3' (forward) and 5'-CTTACACTCTCCACTTTGTG-GTCGGCGGCCGCAAAAGGAAAA-3' (reverse) for photomedin-1; 5'-CCGGAATTCGCCATCATGGCCTATCCCCTGC-CATTG-3' (forward) and 5'-CCTACCATGTCATCTTTGCCT-ACGGCGGCCGCAAAAGGAAAA-3' (reverse) for photomedin-2; 5'-CTCGGATCCACGCCGAGAAGCACACAAGAG-3' (forward) and ATAAGAATGCGGCCGCCGGCTAAGGCGT-CTTTGCATCT-3' (reverse) for albumin–FLAG. The resulting constructs encode photomedins fused with enhanced GFP (EGFP) and 3 × myc tags or a FLAG tag at the C-terminus. A secreted form of GFP containing the signal sequence of Protein C inhibitor [23], designated sGFP, was constructed by inserting the cDNA sequence encoding the signal sequence into the pEGFP-C1 vector (BD Biosciences, San Jose, CA, U.S.A.) at SnaBI/AgeI sites. FLAG-tagged sGFP (sGFP–FLAG) was constructed by inserting the coding sequence for sGFP into pFLAG-CMV5 vector at

SnaBI/NotI sites. These constructs were transfected into 293T or 293F cells using PolyFect (Qiagen, Valencia, CA, U.S.A.) and 293fectin (Invitrogen) respectively. The spent media of transfected 293F cells were recovered 72 h after transfection by centrifugation at 3000 **g** and applied to an anti-(FLAG M2) column pre-equilibrated with 20 mM Tris/HCl, pH 8.0, containing 150 mM NaCl. The column was washed twice with 20 mM Tris/HCl, pH 8.0, containing 1 M NaCl and 1 mM EDTA, and twice with 4 mM Tris/HCl, pH 8.0, containing 150 mM NaCl and 1 mM EDTA, and then bound proteins were eluted with 100 μg/ml FLAG peptide (Sigma) in 4 mM Tris/HCl, pH 8.0, containing 150 mM NaCl and 1 mM EDTA. The eluate was dialysed against PBS and stored at −80 °C until used. Protein concentration was determined using a BCA (bicinchoninic acid) protein assay kit (Pierce, Rockford, IL, U.S.A.).

Production of antibodies against photomedins

To produce antibodies against photomedins, the cDNA fragments encoding amino acid residues 271–362 of photomedin-1 and amino acid residues 239–489 of photomedin-2 were separately amplified by PCR with the following pairs of primers; 5'-CA-CGGATCCGAGAACGAGAACGAGTGGAAGATGGA-3'/5'-TCGAATTCTCACAAGTTGCCTCCTTCTGAA-3' (photomedin-1) and 5'-CACGGATCCCACCCAGAGTATGAAGAA-CG-3'/5'-TCGAATTCTCACCTTCCTATCACATTCCGA-3' (photomedin-2). The PCR products were cloned into pGEX4T1 (Amersham Biosciences). The constructs were transformed into *Escherichia coli* BL21 (Invitrogen). Expression and purification of GST fusion proteins was performed according to the manufacturer's instruction. The purified GST fusion proteins, designated GST–PM1 and GST–PM2, were used as immunogens to raise antisera in rabbits. Antibodies against GST–PM1 and GST–PM2 were affinity-purified on immunogen-immobilized columns after depletion of antibodies against GST on a GST-immobilized affinity column, as described previously [24].

Mouse eye extracts

ICR-mouse eyes were cut into small pieces, suspended in PBS containing 10 mM EDTA, 0.1 mM Pefabloc® (Roche Molecular Biochemicals, Mannheim, Germany), 1 μg/ml pepstatin, 1 μg/ml aprotinin and 1 μg/ml leupeptin, homogenized with a Teflon homogenizer, centrifuged at 8000 **g** for 20 min, and the supernatants used as PBS-soluble fractions. Pellets were solubilized with 50 mM Tris/HCl, pH 8.0, containing 10 mM EDTA, 1 % Triton X-100 and 0.1 mM Pefabloc®, suspended by homogenization, stirred overnight at 4 °C, centrifuged at 8000 **g** for 20 min, and the supernatants used as Triton-soluble fractions.

Immunoblotting

Portions (20 μg) of the proteins were dissolved in SDS/PAGE sample treatment buffer with and without 50 mM dithiothreitol, boiled for 5 min, and subjected to SDS/PAGE using 10–20 % (w/v) polyacrylamide gradient gels. Alternatively, protein samples were treated with the buffer containing 50 mM dithiothreitol and 5 % 2-mercaptoethanol, boiled for 5 min, and incubated overnight at room temperature for completion of disulphide reduction. Separated proteins were electrotransferred to nitrocellulose membranes (Amersham Biosciences), followed by detection of photomedins with specific antibodies (0.1 μg/ml). Bound antibodies were visualized using the horseradish peroxidase-conjugated secondary antibody and an ECL® (enchanced chemiluminescence) detection kit (Amersham Biosciences).

Deglycosylation of recombinant and endogenous proteins

Affinity-purified recombinant photomedins were boiled for 5 min in 50 mM Tris/HCl, pH 7.5, containing 0.1 % SDS, 1 % 2-mercaptoethanol and 10 mM EDTA. After cooling to room temperature, proteins were precipitated with acetone, diluted in 50 mM phosphate, pH 6.5, containing 0.1 % SDS, and then neutralized with 1 % Triton X-100. The protein solutions were treated with 1 unit of PNGase F (peptide:N-glycosidase F), 10 munits of neuraminidase, 0.5 munit of O-glycosidase (Roche Molecular Biochemicals) or the combination thereof, at 37 °C for 12 h, followed by SDS/PAGE and subsequent immunoblotting as described above.

Immunofluorohistochemistry

Tissue specimens were obtained from 10-week-old ICR mice and frozen without fixation. For immunohistochemistry, 7-μm-thick sections were cut, fixed in 4 % paraformaldehyde in PBS, and blocked with PBS containing 10 % FBS for 30 min, and then treated with antibodies against photomedin-1 or -2 (1 μg/ml) overnight at 4 °C. The specimens were treated with appropriate diluted (1:200) fluorophore-labelled secondary antibodies, together with propidium iodide (1:100) for 1 h, washed with PBS, and observed under a Zeiss LSM5 PASCAL confocal laser microscope (Carl Zeiss, Göttingen, Germany).

Assays of solid-phase binding to ECM molecules

Plates (96-well) were coated overnight at 4 °C with the following ECM molecules: 20 μg/ml collagen type I (Nitta Gelatin, Osaka, Japan), type II (Chemicon, Temecula, CA, U.S.A.), type III (Nitta Gelatin), type IV (BD Biosciences), type V (Chemicon), type VI (Chemicon), laminin-1 (Sigma), laminin-2 (human merosin; Chemicon), human laminin-10 (Chemicon), recombinant laminin-10 [a gift from Dr Hironobu Fujiwara at one of our institutions (Sekiguchi Biomatrix Signaling Project, ERATO, Japan Science and Technology Agency)], bovine fibronectin purified from FBS by gelatin-affinity chromatography, proteoglycans from chicken sternum (Elastin Products, Owensville, MO, U.S.A.) and decorin (Sigma); gelatin (100 μg/ml) and Matrigel (500 μg/ml; Sigma); and 20 μg/ml CS-C, CS-D and CS-E, dermatan sulphate, hyaluronic acid, heparan sulphate and heparin, which were conjugated to dipalmitoyl phosphatidylethanolamine [25]. The plates were blocked with 3 % (w/v) BSA in PBS, incubated with purified PM1–FLAG, PM2–FLAG, sGFP–FLAG (negative control), or albumin–FLAG (negative control) for 2 h at room temperature, washed with PBS containing 1 % BSA, and then incubated with horseradish-peroxidase-conjugated anti-(FLAG M2) antibody (Sigma) at 1:1000 dilution at room temperature for 30 min. The bound photomedins were quantified from their absorbance at 490 nm after a colorimetric reaction using O-phenylenediamine and H_2O_2 as substrates.

RESULTS

Screening of RIKEN FANTOM (Functional Annotation of Mouse) cDNAs for novel ECM proteins

We screened the RIKEN FANTOM mouse cDNA sequences for novel ECM proteins by applying the following computational criteria: (1) the presence of a signal sequence at their N-termini and the absence of any transmembrane domains; (2) a size larger than 300 amino acid residues, and (3) novelty in their nucleotide and deduced amino acid sequences. The first criterion extracts

proteins that can be secreted into the extracellular environment, being successfully employed for defining mouse 'secretome', a class of proteins secreted extracellularly [26]. The second criterion was arbitrarily employed to eliminate small secreted proteins, thereby enriching the cDNAs encoding ECM components, whose molecular masses are often in excess of 100 kDa. Through these strategic criteria, we extracted 198 cDNA clones as the candidates for novel ECM proteins from 60770 cDNA entries collected from 246 full-length enriched mouse cDNA libraries (http://genome.gsc.riken.jp). To further select novel ECM proteins, we expressed all these candidate cDNAs in 293T cells as full-length GFP fusion proteins and examined whether the fusion proteins were deposited in any form of ECM, i.e. fibrillar meshworks, basement membrane-like sheets or more restricted dot-like deposits.

Among 40 candidate cDNAs thus selected, two cDNAs yielded dot-like deposits around the transfected cells (see Figure 2 below). These two cDNAs encode novel OLF-family proteins with similar domain structures characterized by the presence of an OLF domain in their C-terminal regions. Since these novel proteins are strongly expressed in the inter-photoreceptor matrix in retina as described below and contain an olfactomedin domain, we coined the name 'photomedins' for these novel OLF domain-containing proteins.

Amino acid sequences and domain structures of photomedins

Photomedin cDNAs have open reading frames encoding 681 and 746 amino acid residues, which are designated photomedin-1 and -2 respectively (Figure 1A). Both proteins have a signal sequence at their N-termini, followed by two tandem CXCXCX₉C motifs, a putative coiled-coil region, a serine/threonine-rich region and an OLF domain in their C-termini (Figure 1B). Photomedin-1 and -2 contain two and three potential N-glycosylation sites respectively. The domain structure of photomedins is similar to that of other OLF-family proteins, including OLF, myocilin, noelin, optimedin/noelin-3, tiarin and amassin (Figure 1B). The overall amino-acid-sequence homologies of the OLF domains between photomedin-1 and the other OLF-family proteins ranges from 69 % (photomedin-2) to 24 % [bullfrog (*Rana catesbeiana*) olfactomedin], as shown in Figure 1B. Two tandem CXCXCX₉C motifs are unique to photomedin-1 and -2 among the known OLF-family proteins, although closely related CXCX₉C motifs are present in noelin, optimedin/noelin-3 and amassin, and shorter CXC motifs are present in OLF and tiarin (Figure 1C). The Ser/Thr-rich region preceding the OLF domain is also unique to photomedins and absent from other OLF-family proteins. This region has been shown to be O-glycosylated in photomedins (see below).

Secretion and ECM deposition of photomedins

To verify the secretion and ECM deposition of photomedins, we expressed photomedin-1 and -2 as GFP fusion proteins in 293T cells. Both photomedin-1 and -2 were predominantly localized within the transfected cells, but were also detected as dot-like aggregates around the cells under non-permeable staining conditions (Figure 2). sGFP, containing the signal sequence of Protein C inhibitor [23], did not give such dot-like deposits, supporting the possibility that photomedin-1 and -2 were secreted and deposited as aggregates around transfected cells.

To further verify that photomedins are secreted proteins, we also expressed photomedin-1 and -2 with a FLAG tag in non-adherent 293F cells. Photomedin-1 and -2 were detected in the medium on immunoblotting (Figure 3A), confirming that they are secreted proteins.
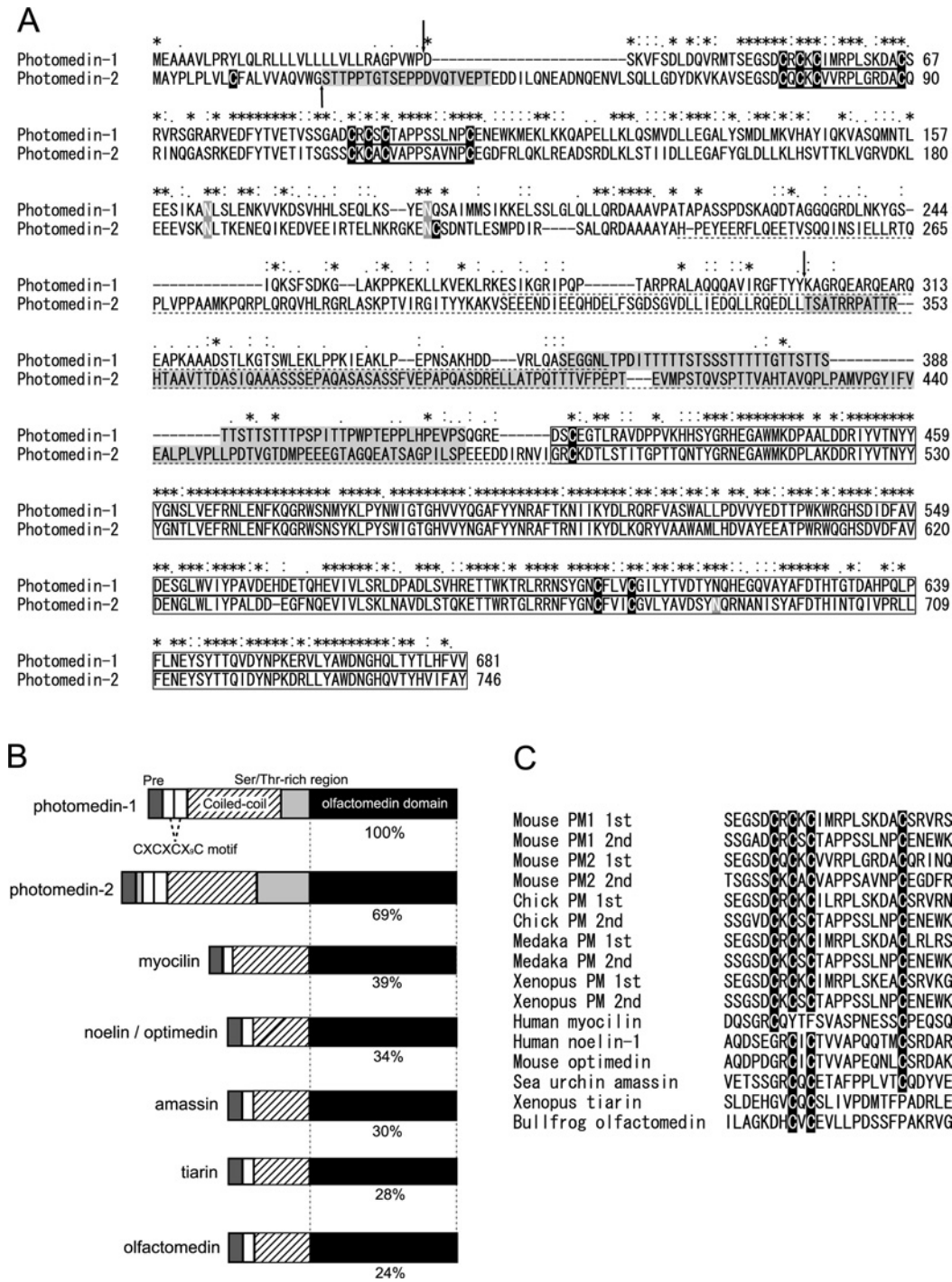
Figure 1 Structures of photomedins

(**A**) Alignment of deduced amino acid sequences of mouse photomedin-1 and -2. Cysteine residues are black-boxed and shown in reverse contrast and CXCXCX₉C motifs are underlined. Amino acid sequences encoding OLF domains are open-boxed. Potential N-glycosylation sites are light-grey-boxed and shown in reverse contrast. Serine/threonine-rich regions are shaded light grey. The sequences used for recombinant production of antigenic fragments are broken-underlined. Residues identical or similar between photomedin-1 and photomedin-2 are marked with asterisks and colons respectively. The cleavage sites deduced by determination of the N-terminal amino acid sequence of purified photomedins are indicated by vertical arrows. (**B**) Schematic domain structures of photomedins and other OLF-family proteins. Signal sequences (labelled 'Pre') and Ser/Thr-rich regions are shaded dark and light grey respectively; regions containing CXC motifs including CXCXCX₉C motifs are indicated by white boxes, coiled-coil domains by hatched boxes, and OLF domains by black boxes. The sequence homologies in OLF domain between photomedin-1 and other OLF-family proteins are shown below each OLF domain. (**C**) Alignment of amino acid sequences containing CXCXCX₉C and related CXC-containing motifs present in photomedins and other OLF-family proteins. The sequences of photomedin orthologues were deduced from expressed-sequence-tag sequences. The first and second CXCXCX₉C motifs of photomedins are separately aligned. The GenBank® accession numbers of the photomedin orthologues are: chick (*Gallus domesticus*) photomedin, AJ393408; Japanese medaka fish (*Oryzias latipes*) photomedin, AU172132; *Xenopus* photomedin, BJ068693.
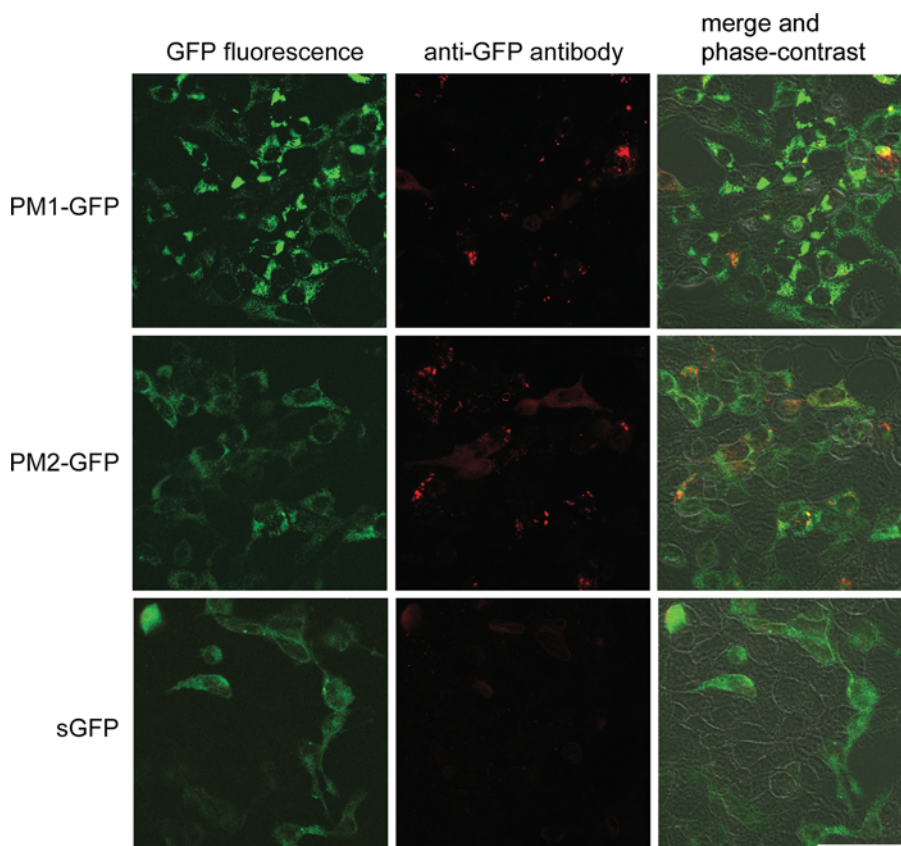
Figure 2   Cellular localization of transiently expressed photomedins

(**A**) Photomedins were expressed as GFP fusion proteins in 293T cells and their subcellular distributions were examined by confocal laser fluorescent microscopy 48 h after transfection. A secreted form of GFP (sGFP) containing the signal sequence of protein C inhibitor [23] was also transfected to 293T cells as a control. GFP fluorescent images are shown in the left column, whereas images obtained by immunofluorescence staining with anti-GFP antibody under non-permeable conditions are shown in the middle column. The centre column shows merged images of left and centre columns along with phase-contrast images. The bar represents 50 μm.

Dimerization/oligomerization and proteolytic processing of photomedins

Upon SDS/PAGE under reducing conditions, photomedin-1 secreted by 293F cells was resolved into 100 and 65 kDa bands (Figure 3A). When resolved under non-reducing conditions, the 65 kDa band remained unchanged, but the 100 kDa band was undetectable; instead, two minor bands migrating at the ≈ 210 and 180 kDa regions were detected, raising the possibility that they were the homodimer of the 100 kDa photomedin-1 and the heterodimer of the 100 kDa photomedin-1 and its 65 kDa fragment respectively. To explore this possibility, photomedin-1 secreted by 293F cells was partially purified by anti-FLAG monoclonal antibody immunoaffinity chromatography and subjected to N-terminal amino acid sequencing. Although because we had limited amounts of the material we could not determine the N-terminal sequence of the 100 kDa protein, the N-terminal sequence of the 65 kDa band was found to be KAGRQEARQE, which corresponded to the sequence of Lys[301]–Glu[310] of the predicted sequence of photomedin-1 (see Figure 1A), indicating that photomedin-1 is proteolytically processed before or after secretion into the medium. To determine when this proteolytic processing occurs, 293F cells transiently expressing photomedin-1 were lysed and immunoblotted with anti-photomedin-1 antibody. Under reducing conditions, photomedin-1 was detected as 85 kDa protein whose N-terminal sequence was found to be

DSKVFSDLDQ after immunoaffinity purification of photomedin-1 from the detergent lysates of transfected 293F cells. This sequence corresponds to Asp[33]–Gln[42] of the predicted photomedin-1, which is immediately after the predicted signal sequence, indicating that the cytoplasmic 85 kDa form represents intact photomedin-1. Under non-reducing conditions, however, photomedin-1 was detected as a 85 kDa band as well as multiple bands migrating at positions corresponding to 245–190 kDa, proteins at the lower molecular mass appearing to represent dimeric forms with different degrees of glycosylation and/or other post-translational modification(s). The absence of any proteolytically processed forms within cytoplasm supports the possibility that the proteolytic processing at the cleavage site Tyr[300]–Lys[301] takes place after secretion from the cells. These results also indicate that photomedin-1 forms disulphide-bonded dimers, possibly through the N-terminal region containing tandem $CXCXCX_9C$ motifs, since the 65 kDa fragment secreted to the medium lacked the N-terminal region and was unable to form disulphide-bonded dimers.

Photomedin-2 secreted to the medium gave two bands at the ≈ 210 and 105 kDa regions upon SDS/PAGE under reducing conditions (Figure 3A). Partial purification and subsequent N-terminal amino acid sequencing revealed that the N-terminal sequence of the 105 kDa band was STTPPTGTSE, which corresponded to Ser[21]–Glu[30] of the predicted sequence of photomedin-2. Thus photomedin-2 was secreted as an intact form after
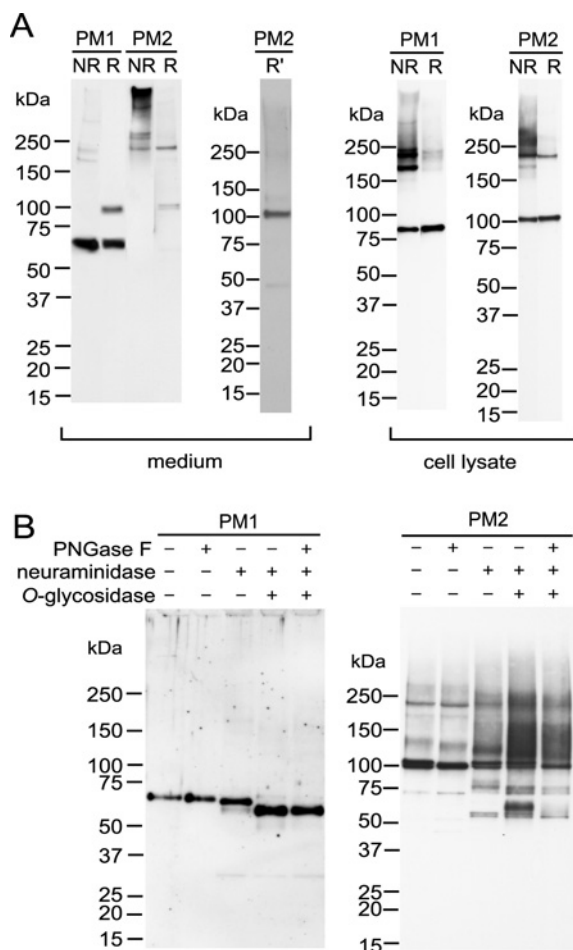
Figure 3 SDS/PAGE and immunoblotting analyses of recombinant photomedins

(**A**) Photomedin-1 (PM1) and photomedin-2 (PM2) were transiently expressed in 293F cells with a C-terminal FLAG tag. Spent medium was collected 72 h after transfection and subjected to SDS/PAGE under reducing (R) and non-reducing (NR) conditions, followed by immunoblotting with antibodies against each protein. For completion of disulphide reduction, spent medium containing recombinant photomedin-2 was also reduced in SDS/PAGE sample treatment buffer containing 50 mM dithiothreitol and 5 % 2-mercaptoethanol, boiled for 5 min, and incubated at room temperature overnight (R′). Cell pellets were lysed in the standard sample treatment buffer with and without a reducing agent (R and NR respectively), boiled for 5 min, and subjected to SDS/PAGE and subsequent immunoblot analyses. Positions of molecular-size markers are shown in the left margin. (**B**) Recombinant photomedins expressed in 293F cells with a FLAG tag were purified from the spent medium harvested 72 h after transfection, as described in the Experimental section. Purified proteins were deglycosylated with PNGase F, neuraminidase, O-glycosidase, or different combinations thereof, and subjected to SDS/PAGE and subsequent immunoblotting under reducing conditions.

removal of its signal sequence. The ≈ 210 kDa band appears to be a dimeric form of the 105 kDa photomedin-2 resulting from incomplete reduction of intermolecular disulphide bonds, since it disappeared on prolonged reduction in the SDS/PAGE sample treatment buffer containing both 50 mM dithiothreitol and 5 % 2-mercaptoethanol. Under non-reducing conditions, photomedin-2 barely entered the gel, indicating that it forms oligomers/multimers stabilized by an interchain disulphide bond(s). When cytoplasmic photomedin-2 was analysed by SDS/PAGE, both the 105 and the ≈ 210 kDa bands were detectable under reducing and non-reducing conditions, although additional broad bands migrating in the 250–300 kDa region were also detected under non-reducing conditions. Taken together, these results indicate

that photomedin-2 is readily assembled into dimers inside cells and forms multimers after secretion.

O-glycosylation of photomedins

Since photomedins have a Ser/Thr-rich region, we examined whether photomedins were O-glycosylated. When photomedin-1 was purified from the conditioned medium of 293F cells and treated with O-glycanase in the presence of neuraminidase, there was a clear decrease in the apparent molecular mass of the 65 kDa band, although neuraminidase treatment alone caused no, or only a small, decrease (Figure 3B). By contrast, PNGase F, which removes *N*-glycans, did not exert any significant effect on the apparent molecular mass of the 65 kDa photomedin-1. Since the 65 kDa photomedin-1 is assumed to contain the N-terminally located Ser/Thr-rich region, these results indicate that photomedin-1 is O-glycosylated at this region.

Immunoblotting of photomedin-2 purified from the conditioned medium of 293F cells gave multiple bands in the 105, 135, 210 and > 250 kDa regions, of which the doublet bands in the 105 kDa region were most prominent (Figure 3B). The upper band in the 105 kDa region was selectively removed by PNGase F treatment with a concomitant increase of the lower band, indicating that the upper, but not the lower, band contained *N*-glycan(s). The lower 105 kDa band was not affected by treatment with neuraminidase alone or neuraminidase plus O-glycanase. These results indicate that the lower 105 kDa band was devoid of O-glycans, representing the unglycosylated form of photomedin-2. Interestingly, the reactivity towards anti-photomedin-2 antibody slightly increased upon treatment with neuraminidase and prominently increased upon treatment with neuraminidase plus O-glycanase, yielding smear bands in the 160–110 kDa region. Since the antigenic fragment used for production of anti-photomedin-2 antibody encompasses the region from His[239] to Arg[490], in which the Ser/Thr-rich region is included, it seems likely that removal of O-glycans attached to the Ser/Thr-rich region potentiates the reactivity of photomedin-2 towards the antibody. The smear bands migrating in the 160–110 and > 200 kDa regions may represent monomeric and dimeric forms respectively of partially O-glycosylated photomedin-2.

Tissue distributions of photomedin-1 and -2

Northern-blot analysis of total RNA isolated from various mouse tissues detected photomedin-1 transcripts as 5 and 3.5 kb RNAs in the lung, eye, testis, non-pregnant uterus and ovary, and, to a lesser extent, in the heart, skeletal muscle, mammary gland, skin and prostate, but not in the brain, thymus, liver, spleen, kidney, submaxillary gland, pancreas and intestine (Figure 4). Detection of two RNA species of different size could be due to alternative splicing of pre-mRNA or presence of alternative transcription start sites. Photomedin-2 transcripts exhibited a similar, but broader spectrum of tissue specificities, being detected as 3.5 kb RNA in the heart, lung, skeletal muscle, mammary gland, skin, stomach, eye, large intestine, testis, epididymis, uterus and ovary, and, to a lesser extent, in the brain, kidney, small intestine, placenta, prostate and submaxillary gland, but not in the liver, spleen, pancreas and thymus.

Expression of photomedins in the eye

Since many OLF-family proteins have been shown to be expressed in the brain and retina, and both photomedins are expressed in the eye, we examined the localization of photomedins in the eye in more detail. When homogenates of adult eyes were analysed by immunoblotting, photomedin-1 and -2 were detected as 50 and 110 kDa bands respectively (Figure 5A). These results indicate
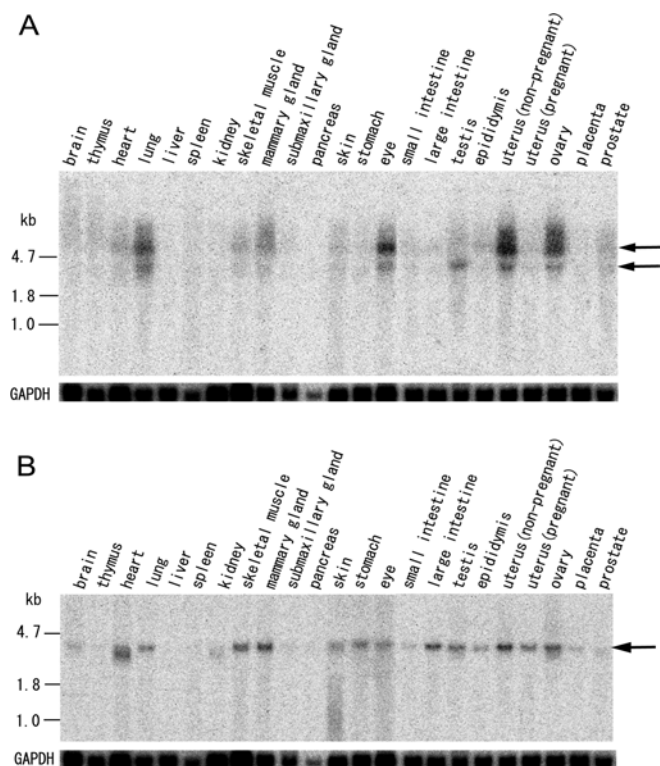
Figure 4   Northern-blot analyses of photomedin transcripts in different mouse tissues

Mouse multiple-tissue Northern blots (upper panels; 20 μg of total RNA per lane) were hybridized with [α-^{32}P]dCTP-labelled cDNA probes for photomedin-1 (**A**) and photomedin-2 (**B**). Blots were stripped and rehybridized with a probe for mouse GAPDH (lower panels). Arrows point to putative photomedin transcripts. Two signals were detected at 5 and 3.5 kb with a probe for photomedin-1.

that photomedin-1 is proteolytically processed in the eye, as was the case with recombinant photomedin-1 expressed in 293F cells, while photomedin-2 is expressed without such processing. The difference in the apparent molecular mass between photomedin-1

extracted from the eye (50 kDa) and recombinant photomedin-1 expressed in 293F cells (65 kDa) could be due to differences in the post-translational modifications, including glycosylation and/or additional proteolytic processing, given that the calculated molecular mass of the fragment encompassing Lys[301]–(C-terminal) Val[681] is 43 kDa – significantly lower than 50/65 kDa.

Immunohistochemistry of retina with anti-photomedin-1 antibody demonstrated that photomedin-1 was predominantly detected in the photoreceptor layers (Figure 5B). Outer nuclear layers as well as outer plexiform layers were also stained, but to a moderate extent. In contrast, photomedin-2 was expressed in ganglion cells, inner nuclear layers especially close to the inner and outer plexiform layers, the inner segment of photoreceptor layers and retinal pigment epithelium. Weak signals were also detected in the inner and outer plexiform layers. Thus the expression patterns of photomedin-1 and -2 appear to be mutually exclusive in the retina.

Binding of photomedins to ECM components

Many ECM molecules are capable of binding to other ECM components, thereby assembling into an intricate supramolecular meshwork structure [27]. To explore the ability of photomedins to bind to other ECM molecules, we developed an ELISA-based high-throughput assay for PM1-FLAG, PM2-FLAG, sGFP-FLAG (negative control), and albumin-FLAG (negative control) binding toward a wide variety of ECM molecules, including various types of collagens, laminins, proteoglycans and glycosaminoglycan chains (Figure 6). Photomedin-1 and -2, both FLAG-tagged, were highly active in binding to CS-E and heparin, but they showed only marginal, if any, binding to other ECM components, i.e., collagens I–VI, laminin-1, -2, and -10, decorin, sternal cartilage proteoglycan and other glycosaminoglycans, including CS-C, CS-D, dermatan sulphate and hyaluronic acid. Heparan sulphate bound only weakly to photomedins. The binding of photomedins to CS-E and heparin was observed under physiological ionic conditions, endorsing its physiological relevance. Neither GFP nor albumin, both FLAG-tagged, exhibited any specific binding to the ECM components, verifying the specificity of photomedin binding to CS-E and heparin (results not shown).
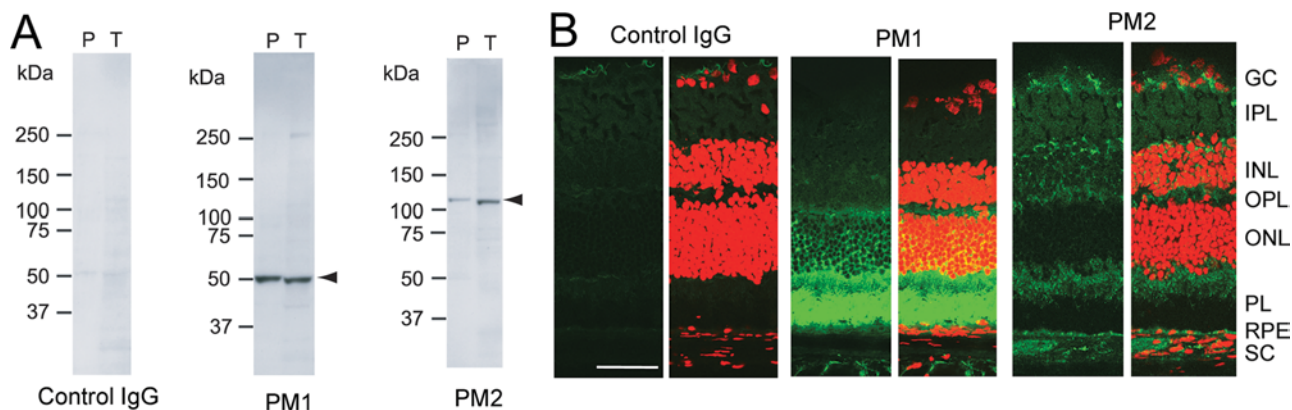

Figure 5   Immunohistochemical localization of photomedins in the retina

(**A**) Immunoblot detection of photomedins in the eye. Adult mouse eyes were sequentially extracted with PBS (P) and 1 % Triton X-100 (T) as described in the Experimental section. The extracts (20 μg of protein) were subjected to SDS/PAGE and subsequent immunoblotting under reducing conditions. Antibodies used were control IgG (left), anti-photomedin-1 (PM1, centre), and anti-photomedin-2 (PM2, right). Arrowheads point to the putative bands of photomedin-1 and -2. (**B**) Immunohistochemical localization of photomedins in the retina. Frozen sections of adult mouse eye were stained by immunofluorohistochemistry using the antibodies against photomedin-1 and -2 (green; left panels). The tissue specimens were also counterstained with propidium iodide (red). Right panels show the merged images for immunofluorescence and propidium iodide staining. GC, ganglion cells; INL, inner nuclear layer; IPL, inner plexiform layer; ONL, outer nuclear layer; OPL, outer plexiform layer; PL, photoreceptor layer; RPE, retinal pigment epithelium; SC, sclera. The bar represents 50 μm.

Photomedin-1
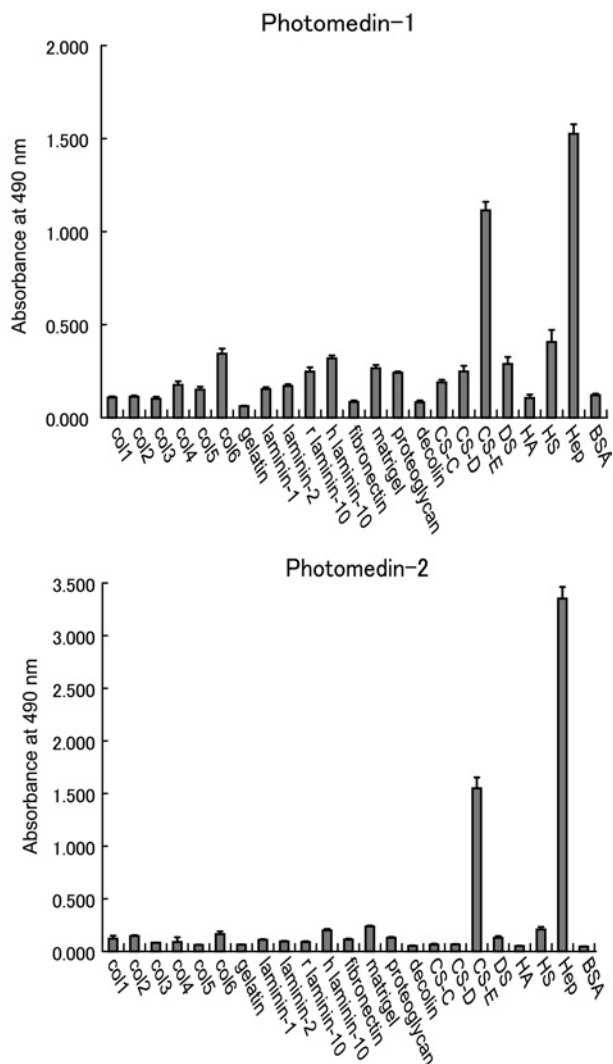

Photomedin-2

Figure 6   Binding of recombinant photomedins to ECM proteins and glycosaminoglycans

Microtitre plates (96-well) were coated with the following ECM proteins or glycosaminoglycans: 20 µg/ml collagens type I, II, III, IV, V and VI (col1, col2, col3, col4, col5, and col6), laminin-1, laminin-2, laminin-10 purified from human placenta (h laminin-10), recombinant laminin-10 (r laminin-10), fibronectin, sternal proteoglycan and decorin, as well as 100 µg/ml gelatin and 500 µg/ml matrigel, and 20 µg/ml CS-C, CS-D, CS-E, dermatan sulphate (DS), hyaluronan (HA) heparan sulphate (HS) and heparin (Hep). Glycosaminoglycans used had been conjugated to dipalmitoyl phosphatidylethanolamine to facilitate their adsorption on to hydrophobic surfaces. Plates were blocked with BSA and incubated with 5 µg/ml of recombinant photomedins with a FLAG tag for 2 h at room temperature, followed by detection of bound photomedins with horse-radish-peroxidase-conjugated anti-FLAG antibody. Bars represent the absorbance at 490 nm. Error bars indicate S.D. ($n = 4$).

DISCUSSION

In the present study we isolated and characterized new members of OLF-family proteins, namely photomedins, from RIKEN's mouse cDNA collections through a combination of computational and functional screenings. Our data show that photomedins (a) are secreted glycoproteins with O-linked carbohydrate chains, (b) are capable of disulphide-bonded dimerization/oligomerization, (c) are able to selectively bind to CS-E and heparin and (d) are expressed in a variety of organs, including retina, where they exhibit mutually exclusive localization patterns. In addition to the

presence of an OLF domain at their C-terminal region, photo-medins are characterized by the presence of the N-terminal signal sequence, CXC-motif-containing regions, and a coiled-coil domain, all of which are shared by other OLF-family proteins.

Despite the similarities between photomedins and other OLF-family proteins, photomedins are unique in that they have $CXCXCX_9C$ motifs repeated in tandem and a Ser/Thr-rich region susceptible to O-linked glycosylation between the coiled-coil and OLF domains. The $CXCXCX_9C$ motif is a variation of the CXC motif commonly found in all OLF-family proteins: amassin, optimedin and noelin have a $CXCX_9C$ motif; *R. catesbeiana* (bullfrog) OLF and *Xenopus laevis* (South African clawed toad) tiarin have a CXC motif, and myocilin has a related $CX_{13}C$ motif (see Figure 1C). Since CXC motifs of OLF-family proteins have been implicated in their disulphide-dependent dimerization/oligomerization [5,7,28], the tandem $CXCXCX_9C$ motifs may also be involved in the dimerization/oligomerization of photo-medins. Our results show that photomedin-1 is synthesized as a disulphide-bonded dimer, but is proteolytically cleaved between Tyr[300] and Lys[301] after secretion from cells, yielding a C-terminal half as a 65 kDa fragment. The 65 kDa fragment is devoid of interchain disulphide bonds, indicating that disulphide-dependent dimerization occurs within the N-terminal half of the molecule, most likely at the tandem $CXCXCX_9C$ motifs. This may also be the case with photomedin-2, although for now we have no solid evidence supporting this possibility. It should be noted that photomedin-2, but not photomedin-1, gives, on SDS/PAGE, a band corresponding to its dimer, even under reducing conditions. This seems to be due to an incomplete reduction of interchain disulphide bonds under the reducing conditions employed, since the band disappeared when the protein was reduced to completion with the sample treatment buffer containing 50 mM dithiothreitol and 5 % 2-mercaptoethanol. Similar partial resistance to reducing agents of interchain disulphide bonds was also reported for bullfrog OLF [28].

Besides the N-terminal $CXCXCX_9C$ motifs, the coiled-coil domain may also be involved in dimerization/oligomerization of photomedins. Coiled-coils are well known motifs capable of di-merization/oligomerization [29,30]. The coiled-coil domain of myocilin has been shown by yeast two-hybrid analysis to possess the ability to self-dimerize [31,32], supporting the possibility that this domain is also involved in dimerization/oligomerization of photomedins. Similarly, the coiled-coil domain is implicated in the dimerization of amassin [5]. The OLF domain *per se* may also be involved in disulphide-dependent dimerization/oligo-merization. Yokoe and Anholt [15] proposed a model in which bullfrog OLF forms multimers through an interchain disulphide bond involving the well-conserved cysteine residue within the OLF domain, although this model remains to be biochemically consolidated.

Although the biological function of most, if not all, OLF-family proteins remain still elusive, it seems likely that their biological activities depend on their oligomer/multimer formation. OLF proteins so far examined have been shown to form disulphide-bonded dimers, as well as oligomers/multimers [3,5,7,28]. Amassin, a sea-urchin plasma protein that mediates massive intercellular adhesion of coelomocytes, was shown to lose its coelomocyte-aggregating activity upon cleavage of interchain disulphide bonds by treatment with 20 mM dithiothreitol [5], underlining the importance of disulphide-dependent multimerization in its bio-logical activity. Disulphide-bonded multimer formation has also been implicated in the role of myocilin in its physiological functions and its involvement in the pathogenesis of primary open-angle glaucoma [33]. Although the functions of photomedins re-main to be elucidated, it is conceivable that disulphide-dependent

dimerization/oligomerization is also required for their biological functions.

A potentially important clue towards uncovering the biological functions of photomedins is their selective binding to CS-E, which is characterized by the presence of 4,6-disulphated *N*-acetyl-galactosamine residues. There is accumulating evidence for the occurrence of CS-E in the brain and for several brain-specific CS proteoglycans, including appican, neurocan, phosphacan and neuroglycan-C [34,35]. It has become clear that CS-E is capable of binding to a panel of heparin-binding growth factors, including midkine, pleiotrophin, FGF (fibroblast growth factor)-2, FGF-10, FGF-16 and FGF-18, and HB-EGF (heparin-binding epidermal growth factor-like growth factor), some of which have been implicated in neuronal-cell migration, axonal guidance in the visual system and neural-cell adhesion [36–39]. These CS-E binding growth factors have been implicated in pathfinding by retinal axons [38]. Given the selective binding of photomedins to CS-E, photomedins may negatively regulate these CS-E-binding growth factors by competing for CS-E. Alternatively, photomedin multimers may serve as reservoir for CS-E-containing CS proteo-glycans, thereby facilitating localized actions of the CS-E-binding growth factors. Since photomedins are also capable of binding to heparan sulphate with a moderate avidity, they may also bind to brain- or nervous-system-specific heparan sulphate proteo-glycans such as agrin, syndecan-2 and syndecan-3, which are also implicated in neuromuscular synaptogenesis [40], spine formation [41] and target recognition of neurites [42] respectively.

In the present study we employed a transcriptome-based screen-ing strategy for identification of new ECM proteins, combining computational screening with a panel of expression screening protocols. RIKEN′s FANTOM mouse cDNA collections cover more than 60000 cDNA clones [43,44], of which about 70 % are full-length, thus ready for *in vitro* expression screening. Since there are no motifs or signature sequences defining ECM proteins, we selected potentially secreted proteins with sizes larger than 300 amino acid residues as the first pool of candidates for new ECM proteins. The candidate clones were expressed in 293T cells and other cell types with a C-terminal GFP tag, followed by examination of their extracellular deposition. We also examined their interactions with a panel of ECM molecules, including glycosaminoglycans, since many ECM proteins have been shown to bind to each other to form supramolecular complexes. Besides photomedins, more than 40 new ECM proteins with distinct spatiotemporal expression profiles have been identified so far (R.-i. Manabe, unpublished work), endorsing our screening strategy. Given the importance of customized ECM around various kinds of tissue parenchymal cells, including stem cells, further characterization of these novel ECM proteins should contribute to a better understanding of the composition and functions of customized ECM in regeneration medicine and tissue engineering.

REFERENCES

1   Bal, R. S. and Anholt, R. R. (1993) Formation of the extracellular mucous matrix of olfactory neuroepithelium: identification of partially glycosylated and nonglycosylated precursors of olfactomedin. Biochemistry **32**, 1047–1053

2   Barembaum, M., Moreno, T. A., LaBonne, C., Sechrist, J. and Bronner-Fraser, M. (2000) Noelin-1 is a secreted glycoprotein involved in generation of the neural crest. Nat. Cell Biol. **2**, 219–225

3   Moreno, T. A. and Bronner-Fraser, M. (2001) The secreted glycoprotein Noelin-1 promotes neurogenesis in *Xenopus*. Dev. Biol. **240**, 340–360

4   Tsuda, H., Sasai, N., Matsuo-Takasaki, M., Sakuragi, M., Murakami, Y. and Sasai, Y. (2002) Dorsalization of the neural tube by *Xenopus* tiarin, a novel patterning factor secreted by the flanking nonneural head ectoderm. Neuron **33**, 515–528

5   Hillier, B. J. and Vacquier, V. D. (2003) Amassin, an olfactomedin protein, mediates the massive intercellular adhesion of sea urchin coelomocytes. J. Cell Biol. **160**, 597–604

6   Kubota, R., Noda, S., Wang, Y., Minoshima, S., Asakawa, S., Kudoh, J., Mashima, Y., Oguchi, Y. and Shimizu, N. (1997) A novel myosin-like protein (myocilin) expressed in the connecting cilium of the photoreceptor: molecular cloning, tissue expression and chromosomal mapping. Genomics **41**, 360–369

7   Nguyen, T. D., Chen, P., Huang, W. D., Chen, H., Johnson, D. and Polansky, J. R. (1998) Gene structure and properties of TIGR, an olfactomedin-related glycoprotein cloned from glucocorticoid-induced trabecular meshwork cells. J. Biol. Chem. **273**, 6341–6350

8   Torrado, M., Trivedi, R., Zinovieva, R., Karavanova, I. and Tomarev, S. I. (2002) Optimedin: a novel olfactomedin-related protein that interacts with myocilin. Hum. Mol. Genet. **11**, 1291–1301

9   Sudhof, T. C. (2001) α-Latrotoxin and its receptors: neurexins and CIRL/latrophilins. Annu. Rev. Neurosci. **24**, 933–962

10 Loria, P. M., Hodgkin, J. and Hobert, O. (2004) A conserved postsynaptic transmembrane protein affecting neuromuscular signaling in *Caenorhabditis elegans*. J. Neurosci. **24**, 2191–2201

11 Khvotchev, M. and Sudhof, T. C. (2000) α-latrotoxin triggers transmitter release via direct insertion into the presynaptic plasma membrane. EMBO J. **19**, 3250–3262

12 Alward, W. L., Fingert, J. H., Coote, M. A., Johnson, A. T., Lerner, S. F., Junqua, D., Durcan, F. J., McCartney, P. J., Mackey, D. A., Sheffield, V. C. and Stone, E. M. (1998) Clinical features associated with mutations in the chromosome 1 open-angle glaucoma gene (GLC1A). N. Engl. J. Med. **338**, 1022–1027

13 Fingert, J. H., Heon, E., Liebmann, J. M., Yamamoto, T., Craig, J. E., Rait, J., Kawase, K., Hoh, S. T., Buys, Y. M., Dickinson, J. et al. (1999) Analysis of myocilin mutations in 1703 glaucoma patients from five different populations. Hum. Mol. Genet. **8**, 899–905

14 Stone, E. M., Fingert, J. H., Alward, W. L., Nguyen, T. D., Polansky, J. R., Sunden, S. L., Nishimura, D., Clark, A. F., Nystuen, A., Nichols, B. E. et al. (1997) Identification of a gene that causes primary open angle glaucoma. Science **275**, 668–670

15 Yokoe, H. and Anholt, R. R. (1993) Molecular cloning of olfactomedin, an extracellular matrix protein specific to olfactory neuroepithelium. Proc. Natl. Acad. Sci. U.S.A. **90**, 4655–4659

16 Bertheussen, K. and Seijelid, R. (1978) Echinoid phagocytes *in vitro*. Exp. Cell Res. **111**, 401–412

17 Boolootian, R. A. and Giese, A. C. (1959) Clotting of echinoderm coelomic fluid. J. Exp. Zool. **140**, 207–229

18 Kulkarni, N. H., Karavanich, C. A., Atchley, W. R. and Anholt, R. R. (2000) Characterization and differential expression of a human gene family of olfactomedin-related proteins. Genet. Res. **76**, 41–50

19 Nakai, K. and Horton, P. (1999) PSORT: a program for detecting sorting signals in proteins and predicting their subcellular localization. Trends Biochem. Sci. **24**, 34–36

20 Hirokawa, T., Boon-Chieng, S. and Mitaku, S. (1998) SOSUI: classification and secondary structure prediction system for membrane proteins. Bioinformatics **14**, 378–379

21 Pearson, W. R., Wood, T., Zhang, Z. and Miller, W. (1997) Comparison of DNA sequences with protein sequences. Genomics **46**, 24–36

22 Sambrook, J. and Russell, D. W. (2001) Molecular Cloning: A Laboratory Manual, 3rd edn, Cold Spring Harbor Laboratory Press, Cold Spring Harbor, NY

23 Ichihara-Tanaka, K., Titani, K. and Sekiguchi, K. (1990) Recombinant carboxyl-terminal fibrin-binding domain of human fibronectin expressed in mouse L cells. J. Biol. Chem. **265**, 401–407

24 Koff, A., Giordano, A., Desai, D., Yamashita, K., Harper, J. W., Elledge, S., Nishimoto, T., Morgan, D. O., Franza, B. R. and Roberts, J. M. (1992) Formation and activation of a cyclin E-cdk2 complex during the G1 phase of the human cell cycle. Science **257**, 1689–1694

25 Sugiura, N., Sakurai, K., Hori, Y., Karasawa, K., Suzuki, S. and Kimata, K. (1993) Preparation of lipid-derivatized glycosaminoglycans to probe a regulatory function of the carbohydrate moieties of proteoglycans in cell–matrix interaction. J. Biol. Chem. **268**, 15779–15787

26 Grimmond, S. M., Miranda, K. C., Yuan, Z., Davis, M. J., Hume, D. A., Yagi, K., Tominaga, N., Bono, H., Hayashizaki, Y., Okazaki, Y. and Teasdale, R. D. (2003) The mouse secretome: functional classification of the proteins secreted into the extracellular environment. Genome Res. **13**, 1350–1359

27 Martin, G. R., Kleinman, H. K., Terranova, V. P., Ledbetter, S. and Hassell, J. R. (1984) The regulation of basement membrane formation and cell-matrix interactions by defined supramolecular complexes. Ciba Found. Symp. **108**, 197–212

28 Snyder, D. A., Rivers, A. M., Yokoe, H., Menco, B. P. and Anholt, R. R. (1991) Olfactomedin: purification, characterization and localization of a novel olfactory glycoprotein. Biochemistry **30**, 9143–9153

29 Kammerer, R. A. (1997) α-Helical coiled-coil oligomerization domains in extracellular proteins. Matrix Biol. **15**, 555–565

30 Muller, K. M., Arndt, K. M. and Alber, T. (2000) Protein fusions to coiled-coil domains. Methods Enzymol. **328**, 261–282

31 Wentz-Hunter, K., Ueda, J. and Yue, B. Y. (2002) Protein interactions with myocilin. Invest. Ophthalmol. Visual Sci. **43**, 176–182

32 Fautsch, M. P. and Johnson, D. H. (2001) Characterization of myocilin–myocilin interactions. Invest. Ophthalmol. Visual Sci. **42**, 2324–2331

33 Gong, G., Kosoko-Lasaki, O., Haynatzki, G. R. and Wilson, M. R. (2004) Genetic dissection of myocilin glaucoma. Hum. Mol. Genet. **13**, R91–R102

34 Shuo, T., Aono, S., Matsui, F., Tokita, Y., Maeda, H., Shimada, K. and Oohira, A. (2004) Developmental changes in the biochemical and immunological characters of the carbohydrate moiety of neuroglycan C, a brain-specific chondroitin sulphate proteoglycan. Glycoconj. J. **20**, 267–278

35 Tsuchida, K., Shioi, J., Yamada, S., Boghosian, G., Wu, A., Cai, H., Sugahara, K. and Robakis, N. K. (2001) Appican, the proteoglycan form of the amyloid precursor protein, contains chondroitin sulphate E in the repeating disaccharide region and 4-O-sulphated galactose in the linkage region. J. Biol. Chem. **276**, 37155–37160

36 Deepa, S. S., Umehara, Y., Higashiyama, S., Itoh, N. and Sugahara, K. (2002) Specific molecular interactions of oversulphated chondroitin sulphate E with various heparin-binding growth factors. Implications as a physiological binding partner in the brain and other tissues. J. Biol. Chem. **277**, 43707–43716

37 Maeda, N. and Noda, M. (1998) Involvement of receptor-like protein tyrosine phosphatase ζ/RPTPβ and its ligand pleiotrophin/heparin-binding growth-associated molecule (HB-GAM) in neuronal migration. J. Cell Biol. **142**, 203–216

38 McFarlane, S., McNeill, L. and Holt, C. E. (1995) FGF signaling and target recognition in the developing *Xenopus* visual system. Neuron **15**, 1017–1028

39 Ueoka, C., Kaneda, N., Okazaki, I., Nadanaka, S., Muramatsu, T. and Sugahara, K. (2000) Neuronal cell adhesion, mediated by the heparin-binding neuroregulatory factor midkine, is specifically inhibited by chondroitin sulphate E. Structural and functional implications of the over-sulphated chondroitin sulphate. J. Biol. Chem. **275**, 37407–37413

40 Gautam, M., Noakes, P. G., Moscoso, L., Rupp, F., Scheller, R. H., Merlie, J. P. and Sanes, J. R. (1996) Defective neuromuscular synaptogenesis in agrin-deficient mutant mice. Cell **85**, 525–535

41 Yamaguchi, Y. (2002) Glycobiology of the synapse: the role of glycans in the formation, maturation and modulation of synapses. Biochim. Biophys. Acta **1573**, 369–376

42 Inatani, M. and Tanihara, H. (2002) Proteoglycans in retina. Prog. Retinal Eye Res. **21**, 429

43 The RIKEN Genome Exploration Research Group Phase II Team, and the FANTOM Consortium (2001) Functional annotation of a full-length mouse cDNA collection. Nature (London) **409**, 685–690

44 The FANTOM Consortium, and the RIKEN Genome Exploration Research Group Phase I and II, Team (2002) Analysis of the mouse transcriptome based on functional annotation of 60 770 full-length cDNAs. Nature (London) **420**, 563–573